

ORGANISATION EUROPEENNE POUR LA RECHERCHE NUCLEAIRE
EUROPEAN ORGANIZATION FOR NUCLEAR RESEARCH
1211 Geneve 23, Switzerland

CLIC Note 425
09 December 1999

Beam Loading Compensation of the CTF II Drive Beam using Idle Cavities

Staffan Rosander

Alfvén Laboratory, KTH, Stockholm

Marco Valentini & Hans Braun

CERN, PS/LP, Geneve, Switzerland

A pair of idle cavity structures has been built at the Alfvén Laboratory, KTH, Stockholm for a second order compensation of the drive beam energy spread in the CLIC Test Facility II (CTF II) at CERN, Geneve. In this note, the theoretical background and the cavity design, together with the experimental results, are presented.

1. Beam-loading compensation in the CLIC Test Facility II

The CLIC Test Facility (CTF) is a prototype two-beam accelerator, in which a high-current “drive beam” is used to generate the RF power for the main-beam accelerator. The CTF II is described in [1] and [2] and some operational parameters of the CTF II drive-beam injector are presented in Table 1.

The drive-beam accelerator consists of two S-band structures which accelerate a bunch train of 48 bunches with a total charge of about 500 nC during 16 ns. The CTF drive-beam train extracts about 1 GW of power from the 3 GHz accelerating structures. This is far more than the power input to the accelerators. The related energy has to be provided by the energy stored in the structures and the heavy beam-loading has to be compensated.

The effect of this substantial beam-loading is compensated for by operating the two accelerating structures at 7.81 MHz above and below the bunch repetition frequency, respectively. This introduces a change of RF phase from bunch to bunch, which leads, together with off-crest injection into the accelerator, to an approximate compensation of the beam loading. Due to the sinusoidal time-dependency of the RF field, an energy spread of about 7% remains in the bunch train. The drive beam energy profile after acceleration has a parabolic profile with the leading and trailing bunches having the same energy and the central bunches having a higher energy.

In the CTF II, simultaneously to acceleration and beam-loading compensation, the drive beam injector has to provide a way to establish the proper single-bunch energy-phase correlation required for magnetic bunch compression. The single-bunch energy-phase correlation can be controlled by using two accelerating structures, one operated at a frequency

higher and the other at a frequency lower than the bunch repetition frequency. By running the two accelerators at the same field amplitude and injecting the train at opposite phase, the single-bunch energy spread introduced in the first structure is compensated by the second one. However, by using the correct phasing and a reduction of the field amplitude in the second structure, it is possible to introduce the same energy-phase correlation in all bunches.

A detailed description of the beam-loading compensation system and of the hardware used is given in [3], [4], [5] and [6].

Table 1. Typical Operational Parameters of the Drive-Beam Injector.

Number of bunches	48	Accelerating Field	35 MV/m
Bunch spacing	10 cm	Residual train energy spread after acceleration	~ 7%
Bunch train charge	500 nC	Correlated single bunch energy spread	~ 7%
Energy	35 MeV	Bunch length after compression (FWHM)	5 ps

2. Idle Cavities

To further reduce the train residual energy spread, a pair of 3-cell idle cavities has been constructed at the Alfvén Laboratory, KTH, Stockholm. The cavities are tuned at frequencies 31.2 MHz higher and lower than the bunch repetition frequency. Due to this frequency difference, the beam-loading of the individual drive beam bunches does not add in phase along the train. It is maximum after 24 bunches, i.e. in the middle of the 48 bunch train, and it is 90° out of phase for the last bunch. This way, the energy of the central part of the train is lowered while the first and last bunch experience only their own wake. As a result, the residual energy spread is further decreased. The idle cavity design has been optimised to reduce the train energy spread to less than 3% at the nominal charge. This is of the same order of the energy spread expected from high order modes.

The use of two cavities tuned at 31.2 MHz above and below the bunch repetition frequency allows to conserve the energy-phase correlation of individual bunches.

2.1 Design Criteria of the Idle Cavities

As the bunch length after acceleration is shorter than 10 ps (FWHM), while the idle cavity resonant period is about 333 ps, the bunches can be regarded as infinitely short. Thus the deceleration of the n -th bunch can be written as:

$$-\Delta W_n = 2k_0q \left\{ \frac{1}{2} + \sum_{m=1}^{n-1} \cos \left(2\pi \frac{\Delta f}{f_b} m \right) \right\} \quad (1)$$

where q is the bunch charge, Δf is the frequency difference between resonant frequency, f_0 , and bunch repetition frequency, f_b , and the loss factor, k_0 , is $k_0 = R/Q^* \omega/4$, where R is the shunt impedance (linac convention), Q is the quality factor and $\omega = 2\pi f_0$.

Employing the relation

$$\sum_{j=0}^k \cos(jx) = \frac{1}{2} \left\{ 1 + \frac{\sin\left(\left(k + \frac{1}{2}\right)x\right)}{\sin\left(\frac{x}{2}\right)} \right\} \quad (2)$$

equation (1) reads

$$-\Delta W_n = k_0 q \frac{\sin\left((2n-1)\pi \frac{\Delta f}{f_b}\right)}{\sin\left(\pi \frac{\Delta f}{f_b}\right)} \quad (3)$$

For the last bunch, $n = 48$, this expression should take the same value as for the first one, i. e. $-\Delta W_{48} = -\Delta W_1$, thus:

$$\sin\left(95\pi \frac{\Delta f}{f_b}\right) = \sin\left(\frac{\Delta f}{f_b}\right) \quad (4)$$

which is fulfilled in the following cases:

$$95\pi \frac{\Delta f}{f_b} = \begin{cases} 2\pi k + \pi \frac{\Delta f}{f_b} & k = 0, 1 \dots \\ (2k+1)\pi - \pi \frac{\Delta f}{f_b} & k = 0, 1 \dots \end{cases} \quad (5)$$

The simplest, non-trivial, solution gives

$$95\pi \frac{\Delta f}{f_b} = 1 - \frac{\Delta f}{f_b} \quad (6)$$

or

$$\Delta f = \pm \frac{f_b}{96} = \pm 31.23 \text{ MHz}$$

and so the idle cavity frequencies were chosen 2967.32 and 3029.78 MHz, respectively. It is interesting to note that the necessary off-frequency, Δf , depends only on the number of bunches in the bunch train and not on the beam intensity. This has the unavoidable consequence that the effectiveness of the idle cavities is limited to the operation at the design bunch train length.

Choice of the Shunt Impedance

On the other hand, the drive beam intensity does determine the level of compensation introduced by the idle cavities. It is clear from Eq. (3) that the deceleration scales linearly with the bunch charge.

The highest correction according to Eq. (3) occurs for bunches 24 and 25,

$$-\Delta W_{24,25} \approx k_0 q \left\{ \frac{\sin \frac{\pi}{2}}{\sin \frac{\pi}{96}} \right\} = 30.55 * k_0 q \quad (8)$$

and the lowest one for bunches 1 or 48,

$$-\Delta W_1 = -\Delta W_{48} = k_0 q \quad (9)$$

For the typical operation conditions presented in Table 1, the bunch charge, q , approximately equals 500/48 nC. The residual energy spread, 7% of 35 MeV \approx 2.45 MeV, is totally compensated by the difference between Eq. (8) and (9), i.e. 29.55* k_0 * q . This is achieved for a total loss factor $k_0=8$ V/pC, which corresponds to a total R/Q of the idle cavities of:

$$\frac{R_{sh}}{Q_0} = \frac{4k_0}{\omega} = \frac{4 * 2.45 \text{ MeV}}{\omega * q * 29.55} = 1700 \Omega \quad (10)$$

In order to allow operation at bunch train charges higher than 500 nC, it has been decided to limit the compensation level and to accept a residual energy spread of 3-4% for a bunch train charge of 500 nC. This corresponds to a total loss factor of 4 V/pC and to a total R/Q of 850 Ω .

Electric field in the Idle Cavities

It is worthwhile to note that while the decelerating field experienced by the n -th bunch is maximum at the center of the bunch train, the electric field in the idle cavities reaches a maximum at the end of the bunch train. The average electric field after the n -th bunch is:

$$E_n = 2 \frac{k_o}{L} q \sum_{j=1}^n e^{i \frac{2\pi \Delta f}{v} (j-1)} \quad (11)$$

where k_o is the loss factor in the idle cavity, L is the length of the idle cavity, q is the bunch charge, Δf is the idle-cavity off-frequency and f is the bunch repetition frequency.

Figure 1 shows the real and imaginary part and the modulus of the field as in Eq (11). It is clear that the decelerating field is maximum in the middle of the bunch train and that it vanishes for the first and last bunch. The maximum field occurs in the cavity at the end of the train and, for a bunch train charge of 500 nC, it is about 9 MV/m.

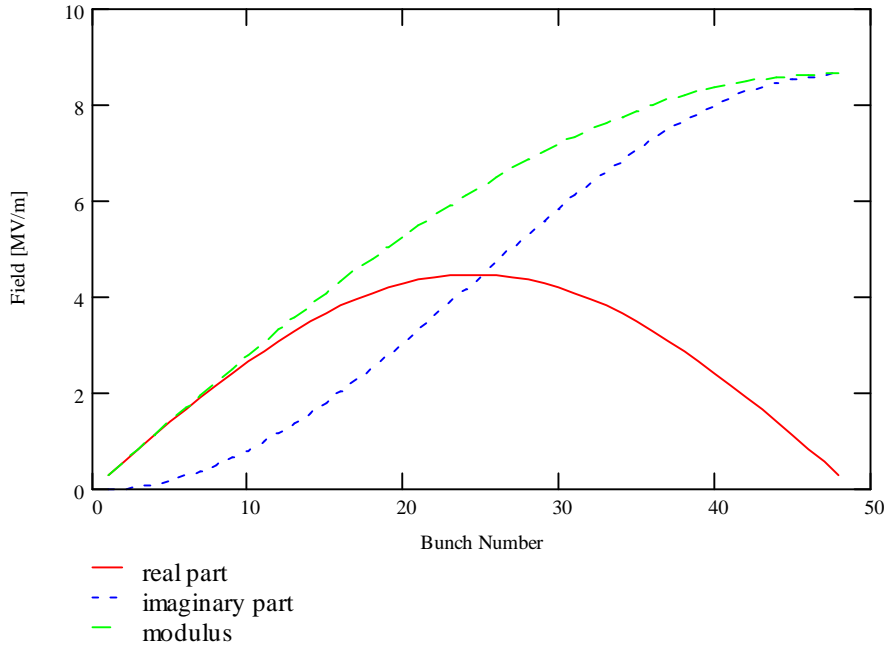


Figure 1. Electric field in the idle cavities as a function of the bunch number along the train. Maximum deceleration occurs in the middle of the train.

2.2 Design and Test of the Idle Cavities

A pair of 3-cell OFHC copper cavities were designed [7], constructed and tested at the Alfvén Laboratory with dimensions according to URMEL calculations performed at CERN. The main design parameters are reported in Table 2. The cavity geometry is shown in Figure 2, the high frequency cavity is on the left side (i.e. the three far left cells) and the low frequency cavity on the right (i.e. the three far right cells).

Table 2. Design and Measured parameters of the Idle Cavities

	High Frequency Cavity		Low Frequency Cavity	
	<i>Design</i>	<i>Measured</i>	<i>Design</i>	<i>Measured</i>
Frequency	3029.78 MHz	3030.09 MHz at 23 °C	2967.32 MHz	2967.72 MHz at 23 °C
		3029.75 MHz extrapolated at 30 °C		2967.37 MHz extrapolated at 30 °C
Qo		just above 12000		just below 12000
R/Qo	425	490 ± 30	425	475 ± 30
Number of cells	3			
ko per cell	0.68 V / pC cell		0.68 V / pC cell	
L of a cell	0.05 m/cell			
mode	π			

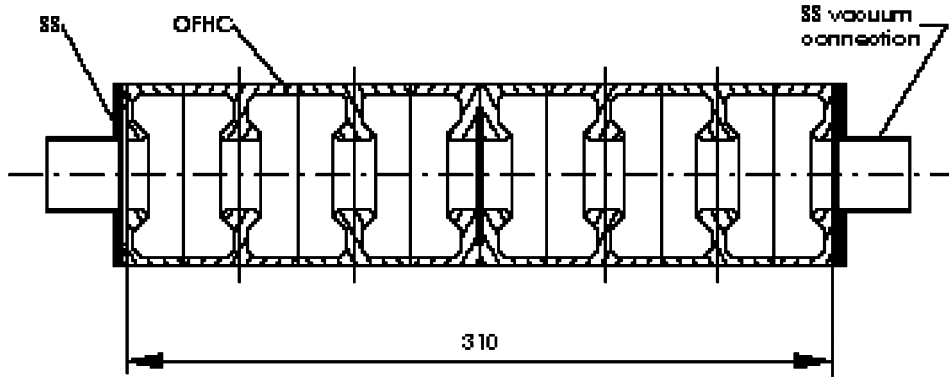


Figure 2. Idle cavity cross section

The measurements and the calculations revealed a coupling constant, k , of 7.39 and 7.03 per mille for the high and low frequency cavities, respectively. Therefore, the outer cells were given respectively 5.56 and 5.25 MHz higher proper frequency (f_{out}) than that of the corresponding middle cell (f_{mid}). In the π -mode, the coupled reactances thereby give each of the three cells of either cavity the same resonant frequency [8]

$$f_{\pi} = \frac{f_{out}}{\sqrt{1 - k/2}} \tag{12}$$

$$f_{\pi} = \frac{f_{mid}}{\sqrt{1 - k}} \tag{13}$$

Thus, in this mode, all three r.f. field amplitudes of each cavity are expected to be equal.

After pre-trimming and brazing of the cavity cells, only a slight change of the cell gap lengths remains to finally set the cell frequencies. This was done by moving the partition walls of the cavity assembly into position with an expandable special tool.

The measured parameters (at 23°C) of the idle cavities are presented in Table 2. The cavities match well the design specifications. The R/Q values, given in Table BB, were found via perturbation technique measurement of the electric field on axis [9]. The measured field distribution is shown in Figure 3, in which the two halves were measured at different frequencies.

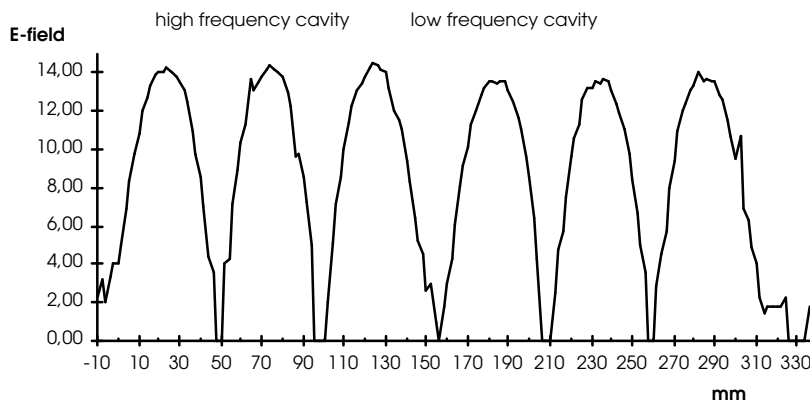


Figure 3. Idle cavities, axial E-field distribution in arbitrary units.

4. Operation

The installation of the beam-loading compensation system has been completed at the beginning of 1998 and the idle cavities have been installed at the beginning of 1999. Despite the fact that the 3 GHz accelerating structures have been conditioned to only 36 MV/m instead of the design value of 60 MV/m, the beam-loading compensation system worked as predicted by the theory. Its flexibility allowed operation at high current levels, which enabled demonstration of the two-beam accelerator scheme [2].

Figure 4 shows a longitudinal phase-space image of a 24 bunch train with a total charge of 120 nC. The measurement has been taken before the installation of the idle cavities. The longitudinal phase space has been measured with a streak camera from a transition radiation screen in a spectrometer behind the accelerators. This way the energy spread is translated in position spread. Only 24 bunches are shown because of the limited acceptance of the streak-camera.

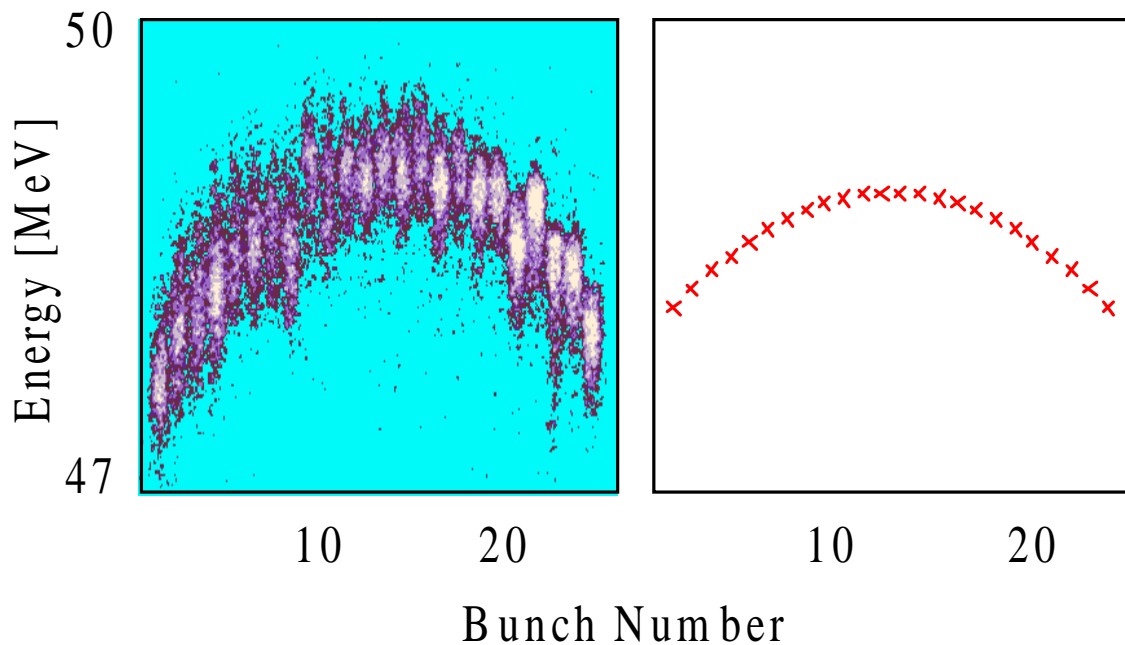


Figure 4. Longitudinal phase space with beam-loading compensation before the installation of the idle cavities. Left side: measured; right side: predicted.

Figure 5 shows the longitudinal phase space of the bunch train after the installation of the idle cavities in case of a train charge of 200 and 50 nC, respectively. Only the central part (i.e. 40 bunches) of the bunch train is visible, due to the limited acceptance of the streak camera. As expected, the residual energy spread decreases as a function of the bunch train charge.

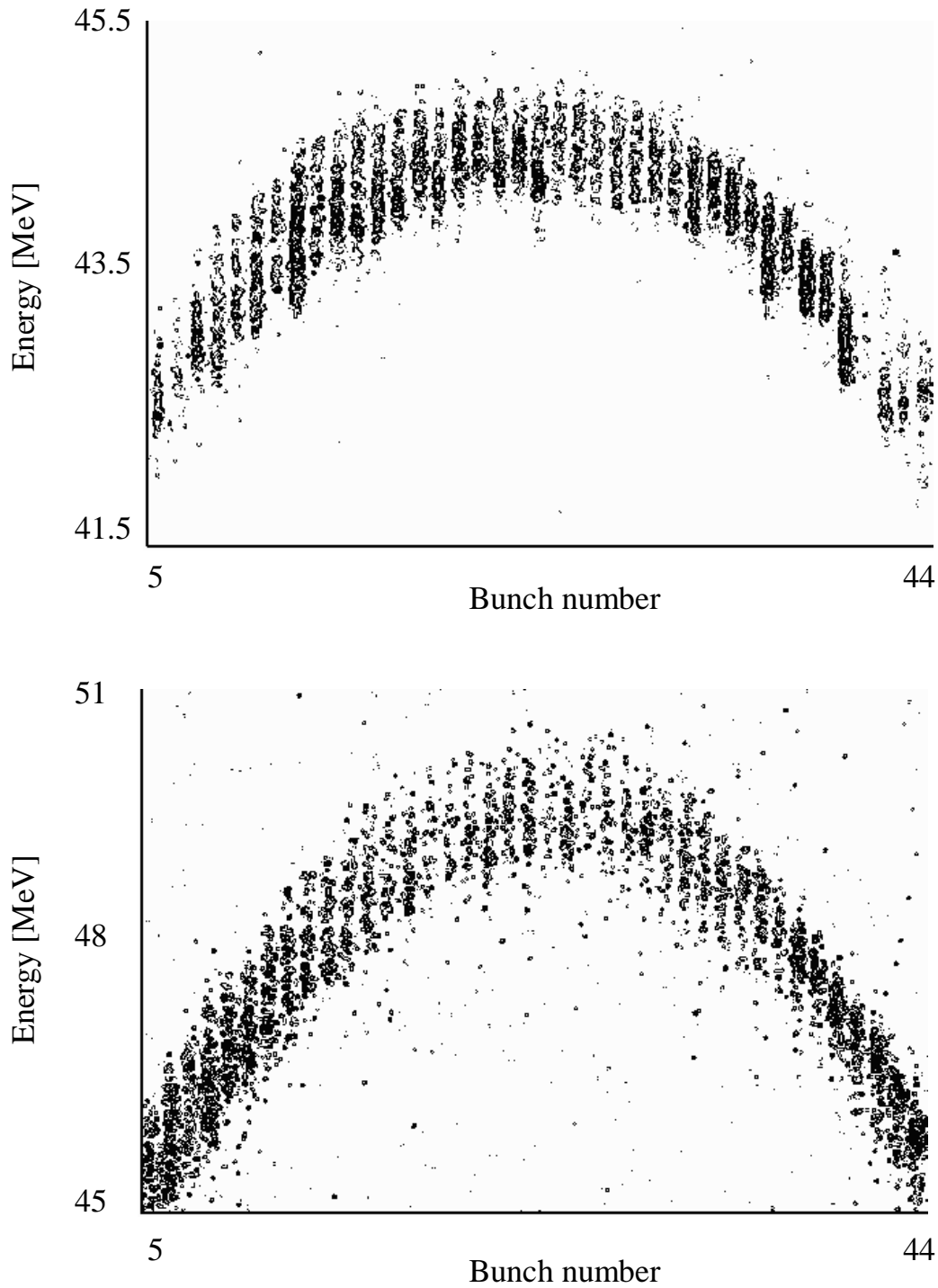


Figure 5. Longitudinal phase space after the installation of the idle cavities. Top: drive beam charge 200 nC, residual energy spread 5.9%. Bottom: drive beam charge 50 nC, residual energy spread 7.2%.

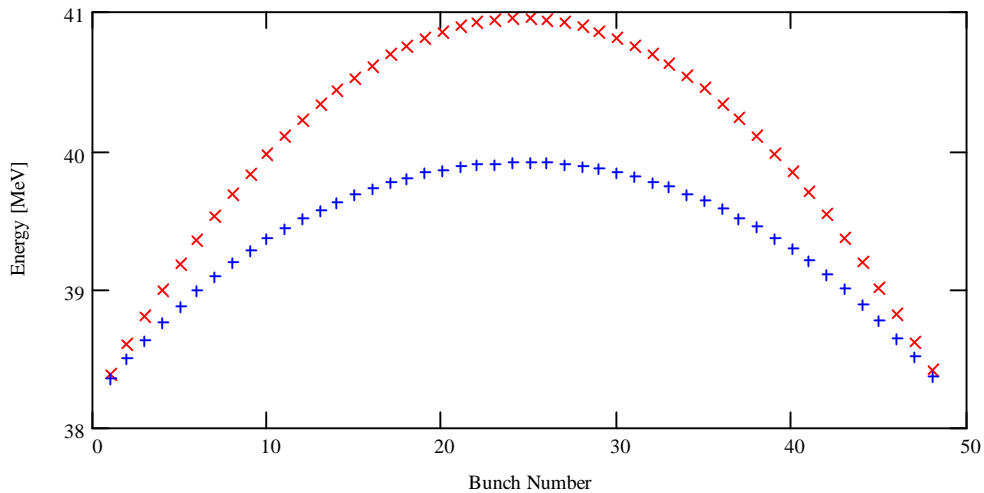


Figure 6. Expected energy distribution along the bunch train with (+) and without (x) the idle cavities. $Q = 400$ nC, no correlation. The total energy spread is reduced to 4%.

Table 3. Idle cavities performance for different bunch charges.

Drive Beam Charge [nC]	Measured Energy Spread [%]	Expected Energy Spread [%]	Measured Energy Min-Max [MeV]	Peak Induced Deceleration field [MV/m]
400	4.3	4	38.3 - 40	7
200	5.8	5.5	42.1 - 44.6	3.5
50	7.4	6.3	45 - 48.5	0.8

Figure 6 shows the expected longitudinal phase space with and without the idle cavities for a drive beam charge of 400 nC (i.e. first case of Table 3).

The measurements are compared with the predictions of the above-reported analytical calculations in Table 3. It is clear that the energy spread reduces with increasing charge as predicted. In addition, there is a very good agreement between measurements and predictions. Without the idle cavities one would expect for the CTF II beam-loading compensation scheme that the energy spread is more or less constant at $\sim 7\%$.

In terms of beam performance, the installation of the idle cavities enabled the transmission of 23% more drive beam charge through the 30 GHz decelerator in comparison with the previous performance. However, in the present CTF II set-up, the drive beam decelerator is twice as long, thus achieving good transmission should be more difficult than in the past.

The idle cavities did not produce any problems with vacuum, electrical break-downs or transverse wakefields.

5. Conclusion

The high transient beam-loading of the CTF drive beam ($\langle I \rangle = 30$ A during 16 ns) has been compensated by adopting a two-frequency beam-loading compensation system. In addition to providing acceleration, the system reduced the total energy spread to 7% and allowed the establishment of single-bunch energy-phase correlation of the order of 1% per degree of bunch phase extension.

The idle cavities performed as predicted and reduced the residual drive beam energy spread depending on the bunch charge. The installation of the idle cavities enabled the transmission of 23% more charge through the 30 GHz decelerator.

References

1. The CLIC Study Group, CTF2 Design Report, CLIC Note 304 and CERN/PS 96-14, 1996.
2. H.H.Braun and 15 co-authors, "Demonstration of Two-Beam Acceleration in CTF II," Proc. Linac '98, Chicago, US and CERN/PS/98-038, 1998.
3. H.H. Braun, M. Valentini, Two-Frequency Beam-Loading Compensation in the Drive Beam Accelerator of the CLIC Test Facility, CLIC Note 390 and CERN/PS 99-016 (LP). Presented at 1999 Particle Accelerator Conference, New York, USA, 28 March - 2 April 1999.
4. M. Valentini, H. Braun, "Analytical Calculation of Beam-Loading Compensation in the High Charge Structures", CERN PS/LP, CTF note 98-05, 19-02-98.
5. M. Valentini, "Interdependence between beam Loading Compensation, Bunch Charge and Energy Gain in HCS", CERN PS/LP, CTF note 97-14,18-09-97.
6. G. Bienvenu, J. Gao, "A Double High Current, High Gradient Electrons Accelerating Structure," Proc. EPAC '96, Sitges, 1996.
7. H.H. Braun and S. Rosander, Resumé of discussion 6 – 7 Nov. 1997 at the Alfvén Laboratory, CTF Note 1997
8. D.E. Nagle, E.A. Knapp, and B.C. Knapp, Coupled Resonator Model for Standing Wave Accelerator Tanks, Rev. Sci. Inst. 38, No. 11 (Nov. 1967) 1583.
9. See e. g. E.L. Ginzton, Microwave Measurements, p. 435 ff., McGraw Hill 1957.